

Age-dependent Preferential Dense-Core Vesicle Exocytosis in Neuroendocrine Cells Revealed by Newly Developed Monomeric Fluorescent Timer Protein

Takashi Tsuboi,^{*†‡} Tetsuya Kitaguchi,^{‡§} Satoshi Karasawa,^{†||} Mitsunori Fukuda,[¶] and Atsushi Miyawaki^{†§}

^{*}Department of Life Sciences, Graduate School of Arts and Sciences, The University of Tokyo, Meguro, Tokyo 153-8902, Japan; [†]Laboratory for Cell Function and Dynamics, Advanced Technology Development Group, Brain Science Institute, RIKEN, Wako, Saitama 351-0198, Japan; [‡]Life Function and Dynamics, Exploratory Research for Advanced Technology, Japan Science and Technology Agency, Wako, Saitama 351-0198, Japan; ^{||}Amalgaam Co., Ltd., Itabashi, Tokyo 173-0004, Japan; and [¶]Laboratory of Membrane Trafficking Mechanisms, Department of Developmental Biology and Neurosciences, Graduate School of Life Sciences, Tohoku University, Sendai, Miyagi 980-8578, Japan

Submitted August 26, 2009; Revised October 13, 2009; Accepted October 28, 2009
Monitoring Editor: Akihiko Nakano

Although it is evident that only a few secretory vesicles accumulating in neuroendocrine cells are qualified to fuse with the plasma membrane and release their contents to the extracellular space, the molecular mechanisms that regulate their exocytosis are poorly understood. For example, it has been controversial whether secretory vesicles are exocytosed randomly or preferentially according to their age. Using a newly developed protein-based fluorescent timer, monomeric Kusabira Green Orange (mK-GO), which changes color with a predictable time course, here we show that small GTPase Rab27A effectors regulate age-dependent exocytosis of secretory vesicles in PC12 cells. When the vesicles were labeled with mK-GO-tagged neuropeptide Y or tissue-type plasminogen activator, punctate structures with green or red fluorescence were observed. Application of high [K⁺] stimulation induced exocytosis of new (green) fluorescent secretory vesicles but not of old (red) vesicles. Overexpression or depletion of rabphilin and synaptotagmin-like protein4-a (Slp4-a), which regulate exocytosis positively and negatively, respectively, disturbed the age-dependent exocytosis of the secretory vesicles in different manners. Our results suggest that coordinate functions of the two effectors of Rab27A, rabphilin and Slp4-a, are required for regulated secretory pathway.

INTRODUCTION

Neuroendocrine cells contain large number of dense-core vesicles that are filled with peptide hormones for secretion. Recent studies have suggested that soluble *N*-ethylmaleimide-sensitive factor attachment protein receptors (SNAREs) (Rothman, 1994; Jahn and Sudhof, 1999) and small GTPase Rabs (Zerial and McBride, 2001) are thought to be required for biogenesis and trafficking of dense-core vesicles. The secretion process (i.e., exocytosis) from neuroendocrine cells of dense-core vesicles consists of 4 steps: 1) the transported

dense-core vesicle morphologically attaches to the plasma membrane (tethering), 2) the tethered vesicle forms a tight core SNARE complex at the target plasma membrane (docking), 3) the preparation of exocytosis competent vesicles depending on Mg²⁺-ATP and temperature (priming), and 4) the fusion of the vesicle with the plasma membrane by extracellular stimuli (fusion). Only a small fraction of these vesicles is able to be released rapidly in response to elevated cytosolic Ca²⁺ concentrations, and this fraction is called the readily releasable pool (RRP). The remaining vesicles are thought to constitute a large cytosolic reserve pool awaiting recruitment into the red fluorescent protein (RRP) for exocytosis. However, the molecular machinery involved in preferential release from RRP (i.e., preferential recruitment of dense-core vesicle to the plasma membrane and its exocytosis) remains largely unknown.

Recently, Duncan *et al.* (2003) revealed, using the vesicle cargo-tagged fluorescent timer protein DsRed-E5 which progressively shifts its fluorescence emission from green to red (Terskikh *et al.*, 2000), that dense-core vesicles segregate into distinct populations based on age in bovine adrenal chromaffin cell. Newly assembled vesicles are immobile and morphologically docked at the plasma membrane shortly after biogenesis, whereas older vesicles are mobile and located deeper in the cells. Furthermore, newly assembled vesicles undergo exocytosis in preference to older vesicles.

This article was published online ahead of print in *MBC in Press* (<http://www.molbiolcell.org/cgi/doi/10.1091/mbc.E09-08-0722>) on November 4, 2009.

† These authors contributed equally to this work.

Address correspondence to: Takashi Tsuboi (takatsuboi@bio.c.u-tokyo.ac.jp) or Atsushi Miyawaki (matsushi@brain.riken.go.jp).

Abbreviations used: HRP, horseradish peroxidase; mK-GO, monomeric Kusabira Green Orange; mKO, monomeric Kusabira Orange; NPY, neuropeptide Y; RRP, readily releasable pool; siRNA, small interfering RNA; Slp, synaptotagmin-like protein; SNAP-25, synaptosome-associated protein of 25 kDa; SNARE, soluble *N*-ethylmaleimide-sensitive factor attachment protein receptor; TIRF, total internal reflection fluorescence; Venus, pH-insensitive yellow.

However, it is not known how the segregation of vesicles according to age is accomplished at the molecular level.

We have recently shown that two small GTPases, Rab3A and Rab27A, are abundantly expressed on the dense-core vesicles and cooperatively regulate the docking step of dense-core vesicle exocytosis in PC12 cells (Tsuboi and Fukuda, 2006a). Furthermore, two Rab3A and Rab27A effector molecules, synaptotagmin-like protein 4-a (Slp4-a, also called granuphilin) and rabphilin, promote dense-core vesicle docking to the plasma membrane (Tsuboi and Fukuda, 2005, 2006b; Tsuboi *et al.*, 2007). Slp4-a and rabphilin share the same domain structures (Cheviet *et al.*, 2004; Fukuda, 2005), but they have opposite effects on exocytosis. Slp4-a has been shown to increase the number of “release-incompetent” vesicles docked to the plasma membrane through interaction with a Munc18-1/syntaxin-1a complex (Gomi *et al.*, 2005; Tsuboi and Fukuda, 2006b; Tomas *et al.*, 2008). In contrast, rabphilin has been shown to increase the number of “release-competent” vesicles docked to the plasma membrane through interaction with synaptosome-associated protein of 25 kDa (SNAP-25) (Tsuboi *et al.*, 2007). These findings lead us to speculate that rabphilin and Slp4-a may regulate segregation of dense-core vesicle recruitment and exocytosis.

In the present study, we investigated the molecular mechanism(s) of preferential dense-core vesicle recruitment and exocytosis in PC12 cells by total internal reflection fluorescence (TIRF) microscopy (Axelrod, 1981) with the vesicle cargo-targeted new fluorescent timer probe monomeric Kusabira Green Orange (mK-GO). Expression of mK-GO-tagged vesicle cargoes in PC12 cells showed that newly assembled vesicles appeared green, those of intermediate age are yellow, and older vesicles are red. Although application of high-KCl stimulation induced newly synthesized dense-core vesicle exocytosis, rabphilin-overexpressing cells showed both newer and older vesicle exocytosis. However, only few exocytotic events were observed in Slp4-a-overexpressing cells. Interestingly, silencing of Slp4-a, by RNA interference-mediated knockdown, resulted in an increase in the number of exocytotic events involving older vesicles. Based on these findings, we propose that Rab27A effectors regulate the preferential release of newly synthesized dense-core vesicle in neuroendocrine cells.

MATERIALS AND METHODS

Protein Expression, In Vitro Spectroscopy, and pH Titrations

Proteins were expressed in *Escherichia coli*, purified, and characterized spectroscopically as described previously (Nagai *et al.*, 2002). For calculation of molar absorption, coefficients and protein concentrations were measured using a Bradford assay kit (Bio-Rad Laboratories, Hercules, CA), with bovine serum albumin as the standard. pH titrations were performed as described previously (Nagai *et al.*, 2002). To analyze the maturation kinetics from green to red, in vitro translation system, WakoPURE system was carried out with the T7 promoter flanking polymerase chain reaction (PCR) products of “fluorescent timer” version of mK-GO at 37°C for 1 h. The synthesized mK-GO was excited at 509 nm and 560 nm, and the ratio of peak amplitudes of fluorescent intensity were plotted against time.

Site-directed Mutagenesis and Plasmid Construction

To develop the monomeric fluorescent timer mK-GO, we introduced six mutations (K49E/P70V/K185E/K188E/S192D/S196G) into wild-type monomeric Kusabira Orange (mKO) (Karasawa *et al.*, 2004; Tsutsui *et al.*, 2005) by site-directed mutagenesis essentially as described previously (Sawano and Miyawaki, 2000). The other plasmids were prepared as described previously (Tsuboi and Fukuda, 2005, 2006b). DNA constructs such as neuropeptide Y (NPY)-mK-GO and tissue-type plasminogen activator (tPA)-mK-GO reported in this article are distributed with concomitant purchase of cDNA for mK-GO from Medical Biological Laboratory International (Amalgaam, Tokyo, Japan).

Slp4-a and Rabphilin Small Interfering RNA (siRNA) and Immunoblotting

To knockdown endogenous Slp4-a and rabphilin protein expression, we used Stealth RNA interference (RNAi) (Invitrogen, Carlsbad, CA) against mouse Slp4-a mRNA (5'-GGGAACAAAGUGUGUGUU-3'), mouse rabphilin mRNA (5'-GGAGAUGGUGUGAACCGUU-3'), and matched siRNA negative controls (scramble siRNA). To validate Slp4-a or rabphilin knockdown, 3 μ l of Slp4-a, rabphilin, or scramble siRNA stock (20 μ M) was transfected into PC12 cells, seeded at 1×10^6 cells per 100-mm dish by using Lipofectamine 2000 (Invitrogen). Two days after transfection, PC12 cells were homogenized in a buffer containing 1 ml of 50 mM HEPES-KOH, pH 7.2, 150 mM NaCl, and protease inhibitors (0.1 mM phenylmethylsulfonyl fluoride, 10 μ M leupeptin, and 10 μ M pepstatin A) in a glass-Teflon Potter homogenizer by 10 strokes at 900-1000 rpm, and the proteins were solubilized with 1% Triton X-100 at 4°C for 1 h. After solubilization with 1% Triton X-100 at 4°C for 1 h, the insoluble material was removed by centrifugation at 15,000 rpm for 10 min. The proteins were analyzed by 12.5% SDS-polyacrylamide gel electrophoresis (PAGE) followed by immunoblotting with anti-granuphilin (Slp4-a) goat polyclonal antibody (1/200 dilution; Santa Cruz Biotechnology, Santa Cruz, CA), anti-rabphilin goat polyclonal antibody (1/100 dilution; Santa Cruz Biotechnology), and anti-actin mouse monoclonal antibody (1/200 dilution; Millipore Bioscience Research Reagents, Temecula, CA). Immunoreactive bands were visualized with horseradish peroxidase (HRP)-conjugated donkey anti-mouse immunoglobulin (Ig)G (1/5000 dilution; Santa Cruz Biotechnology) or HRP-conjugated rabbit anti-goat IgG (1/5000 dilution; Santa Cruz Biotechnology) and detected by enhanced chemiluminescence (GE Healthcare, Little Chalfont, Buckinghamshire, United Kingdom).

TIRF Microscopy

PC12 cells were cultured in DMEM (Invitrogen) supplemented with 10% fetal bovine serum, 10% horse serum, 100 U/ml penicillin G, and 100 μ g/ml streptomycin, at 37°C under 5% CO₂. For TIRF imaging, PC12 cells were plated onto poly-L-lysine-coated coverslips, and the cells were transfected with 4 μ g of NPY-mK-GO or tPA-mK-GO plasmids by using Lipofectamine 2000. To knockdown endogenous Slp4-a or rabphilin protein expression, we cotransfected with 3 μ l of Slp4-a or rabphilin siRNA stock (20 μ M) and either 3 μ g of NPY-mK-GO or tPA-mK-GO vectors into PC12 cells. In contrast, to observe the effect of overexpression of Slp4-a or rabphilin on exocytosis, we cotransfected with 2 μ g of pEF-T7-Slp4-a or pEF-T7-rabphilin and either 2 μ g of NPY-mK-GO or tPA-mK-GO constructs. The cells were used for experiments in 48 h after transfection. The imaging was performed in a modified Ringer's buffer at 37°C (RB: 130 mM NaCl, 3 mM KCl, 5 mM CaCl₂, 1.5 mM MgCl₂, 10 mM glucose, and 10 mM HEPES, pH 7.4). High-KCl stimulation was achieved by perfusion with 70 mM KCl containing RB (the NaCl concentration was reduced to maintain the osmolarity).

To observe the exocytosis of NPY-mK-GO or tPA-mK-GO at the single vesicle level, we used a dual-color TIRF microscope (Tsuboi *et al.*, 2000, 2004, 2007; Tsuboi and Rutter, 2003; Varadi *et al.*, 2005; Tsuboi and Fukuda, 2006b). We mounted a high numerical aperture objective lens (Plan Apochromatic, 100 \times , numerical aperture = 1.45, infinity corrected; Olympus, Tokyo, Japan) on an inverted microscope (IX71; Olympus), and we introduced an incident light for total internal reflection illumination through the high numerical aperture objective lens via a single mode optical fiber and two illumination lenses (IX2-RFAEVA-2; Olympus). To excite the mK-GO probes, we used a diode-pumped solid state 488 nm (HPU50100, 20 mW; Furukawa Electronic, Chiba, Japan) and 561 nm laser (85YCA020, 20 mW; Melles Griot, Tokyo, Japan) for total internal fluorescence illumination. For simultaneous imaging of red and green fluorescence, an image splitter (Dual View; Optical Insights, Santa Fe, NM) divided the red and green components of the images with a 565 nm dichroic mirror (Chroma Technology, Rockingham, VT) and passed the red component through a 580 nm long pass filter (Chroma Technology) and the green component through a 500–540 nm bandpass filter (Chroma Technology). The images were then projected side-by-side onto an electron multiplier charge-coupled device (EM-CCD) camera (C9100-02; Hamamatsu Photonics, Hamamatsu, Japan). The laser beams were passed through an electromagnetically driven shutter (VMM-D3J; Unibriz, Rochester, NY), and the shutter was opened synchronously with EM-CCD camera exposure controlled by MetaMorph software version 7.5 (Molecular Devices, Sunnyvale, CA). Images were acquired every 300 ms or otherwise as indicated.

To analyze the TIRF imaging data, single exocytotic events were selected manually, and the average fluorescence intensity of an individual vesicles in a 0.7- \times 0.7- μ m square placed over the vesicle center was calculated (Tsuboi and Fukuda, 2006a,b, 2007; Tsuboi *et al.*, 2007). To distinguish between fusion events and vesicle retreated, we focused on fluorescence changes just before the disappearance of fluorescent signals. When there was a fusion event, a rapid transient increase in fluorescence intensity (to a peak intensity 1.5 times greater than the original fluorescence intensity within 1 s) was observed, whereas when vesicles moved, the fluorescence intensity gradually decreased to the background level as described previously (Tsuboi and Fukuda, 2006b). The number of fusion events during a 5-min period was counted manually. Data are reported as means \pm SE of at least 25 individual experiments. Statistical significance and differences between means were compared by

one-way analysis of variance followed by the Newman–Keuls multiple comparison test with Prism software (GraphPad Software, San Diego, CA).

RESULTS

Biochemical and Spectral Properties of Fluorescent Timer mK-GO

We previously generated a monomeric version of Kusabira Orange, mKO, from dimer version of wild-type Kusabira Orange fluorescent protein (KO) by introducing mutations in binding surface (Karasawa *et al.*, 2004). During the process of developing brighter and more soluble mutant of mKO, we found a mutant mKO displaying an intermediate green fluorescence transiently in the course of chromophore maturation. We therefore performed additional mutagenesis and finally obtained a color change version (i.e., fluorescent timer) of mKO molecule. In the mKO-base timer fluorescent protein, six mutations (K49E, P70V, K185E, K188E, S192D, and S196G) were eventually introduced into mKO. Then, we named this molecule as a monomeric fluorescent timer version of Kusabira Green Orange or mK-GO.

We analyzed the spectral properties of purified recombinant mK-GO protein prepared from bacteria. The absorption spectrum of mK-GO at pH 7.4 displayed two peaks, one peak at 500 nm ($\epsilon = 35,900 \text{ M}^{-1} \text{ cm}^{-1}$) and one peak at 548 nm ($\epsilon = 42,000 \text{ M}^{-1} \text{ cm}^{-1}$) at pH 7.4 (Figure 1A). The absorption spectrum of mK-GO was slightly and modestly pH-sensitive; the apparent pK_a was determined to be ~ 6.0 and 4.8 at absorbance of 500 nm and 548 nm, respectively (Figure 1B). Excitation and emission spectra of mK-GO are shown in Figure 1C. After excitation at 500 nm or 548 nm, the protein emitted a green or red, peaking at 509 nm or 561 nm, respectively. We next determined the time course of fluorescence maturation in synthesized mK-GO protein by *in vitro* translation (Figure 1D). The ratio of orange per green fluorescence was lineally increased and reached at plateau at ~ 10 h. The time for the half-maximal fluorescence development is ~ 6 h which is faster than DsRed-based fluorescent timer (Terskikh *et al.*, 2002). Together, these results suggest that mK-GO is a monomeric version of fluorescent timer that is suitable for monitoring the age of the targeting protein.

NPY- and tPA-mK-GO Overexpressing PC12 Cells Show Punctate Structure with Green and Red Fluorescence

To examine the relationship between dynamics of the dense-core vesicle exocytosis and its age, we first generated DsRed-E5-tagged neuropeptide Y (NPY-timer) (Terskikh *et al.*, 2000). Although previous study has shown that DsRed-E5-tagged atrial natriuretic factor (ANF-timer) were targeted to the dense-core vesicles in bovine adrenal chromaffin cells (Duncan *et al.*, 2003), NPY-timer in PC12 cells were localized in both cytosol and vesicles with some aggregates (Figure 2A). The most likely explanation for the low targeting efficiency of NPY-timer in PC12 cells is that the fluorescent timer protein (i.e., DsRed-E5) is a tetramer and therefore could form aggregates through cross-linking with the cargo protein or other proteins when it is fused to the dense-core vesicle cargo proteins (i.e., NPY). When our newly developed monomeric fluorescent timer protein (mK-GO)-tagged NPY and tPA were expressed in PC12 cells, the fluorescence was localized to vesicular structures (Figure 2, B and C) consistent with their reported association with the dense-core vesicle. Moreover, the mK-GO-tagged vesicles in 48 h after transfection showed green and red fluorescence, and the percentage of the newly synthesized green vesicles, intermediate yellow vesicles (green and red), and older red vesicles were ~ 20 , 70, and 10%, respectively (Figure 2D). We

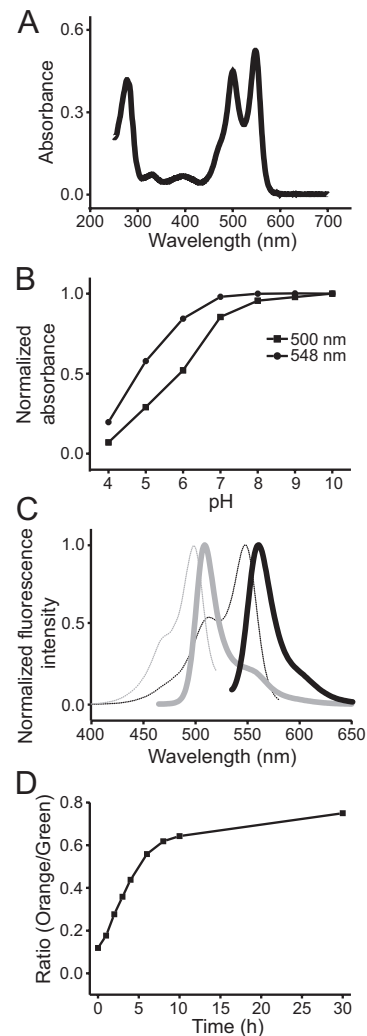


Figure 1. Light-absorption properties and excitation and emission spectra of mK-GO. (A) Absorption spectra of mK-GO. (B) pH dependence of the absorption peak at 500 nm and 548 nm. (C) Normalized excitation (broken line) and emission (solid line) spectra of mK-GO. (D) *In vitro* maturation kinetics: fluorescence emission ratio between 560 nm and 509 nm of freshly synthesized mK-GO were recorded during maturation of the proteins at 37°C.

also observed the time-dependent change in vesicle color from green to red in live PC12 cells at the similar time course as *in vitro*-translated mK-GO (Figure 1 and Supplemental Figures 1 and 2). Therefore, these results suggest that the fusion proteins with the monomeric timer protein, mK-GO do not disturb proper targeting to the dense-core vesicles and retain color timer property to segregate the dense-core vesicles according to its age.

NPY and tPA Are Preferentially Released from Newly Synthesized Dense-Core Vesicles in PC12 Cells

Dense-core vesicles showed green, yellow, and red fluorescence and each fluorescence was implicated as its age: new, intermediate, and old, respectively. To analyze the single vesicle release behavior related to its age, we monitored the dynamics of single exocytotic events within ~ 100 nm beneath the plasma membrane by TIRF microscopy. High-KCl stimulation (70 mM) caused newly synthesized NPY-mK-GO-labeled vesicles (i.e., green vesicles) to brighten and

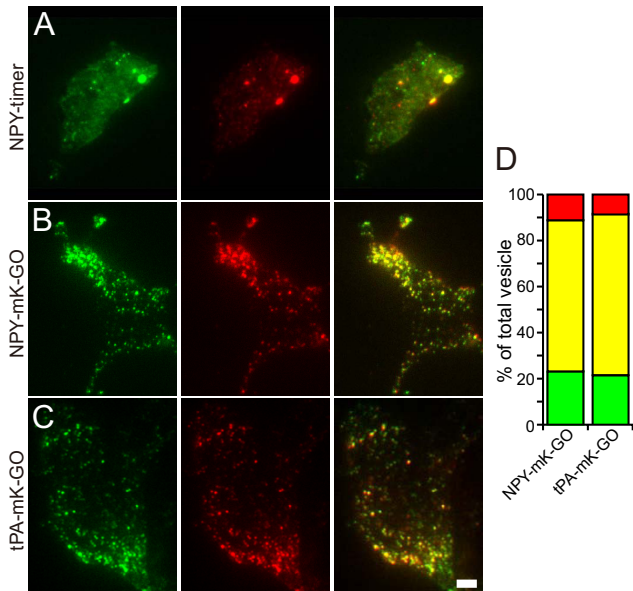


Figure 2. Localization of timer- and mK-GO-tagged dense-core vesicle markers within PC12 cells. TIRF image of PC12 cells showing the distribution of NPY-timer (A), NPY-mK-GO (B), and tPA-mK-GO (C) in 48 h after transfection. Note that the NPY-timer was present throughout the cell cytosol, with the majority located in irregular vesicular structures. (D) Stacked bar chart represents the percent of the number of plasma membrane-docked green, yellow, and red vesicles in NPY- and tPA-mK-GO-expressing cells ($n = 28$ cells in each). Bar, 10 μm .

suddenly spread during release of the fluorescent peptide, with an identical time course in older (i.e., yellow or red) vesicles (Figure 3, A–F). Consistently, tPA-mK-GO-labeled green, yellow, and red vesicles showed similar exocytotic dynamics (data not shown). These data indicated that overexpression of NPY- or tPA-mK-GO in the PC12 cells did not disturb their normal secretory behavior and that the kinetics of new and old vesicle exocytosis were identical.

Because a previous study has shown that the newly assembled dense-core vesicle cargo ANF is preferentially released from bovine adrenal chromaffin cells, we next investigated whether newly synthesized dense-core vesicle cargoes NPY and tPA were also preferentially released from the PC12 cells. To examine preferential vesicle release, we counted the total number of NPY- or tPA-mK-GO release events (i.e., green-, yellow-, and red-colored vesicle exocytosis) during high-KCl stimulation. The mean number of plasma membrane-docked NPY-mK-GO-labeled dense-core vesicles (125 ± 38 vesicles per cells, $n = 31$ cells) was not significantly different from that in cells labeled with tPA-mK-GO (138 ± 25 vesicles per cells, $n = 28$ cells) (Figure 3G), and the ratio of membrane-docked NPY green, yellow, and red vesicles was indistinguishable from that in tPA vesicles (Figure 2D). However, under high-KCl stimulation, very few exocytotic events involving plasma membrane-docked red colored-NPY-mK-GO vesicles were observed (Figure 3, G and H). Similarly, with tPA-mK-GO, which has a larger molecular size than NPY, exocytotic responses were observed mainly from plasma membrane-docked green- and yellow-colored vesicles (Figure 3, G and H). These results suggest that newly synthesized dense-core vesicle cargoes are released preferentially in PC12 cells.

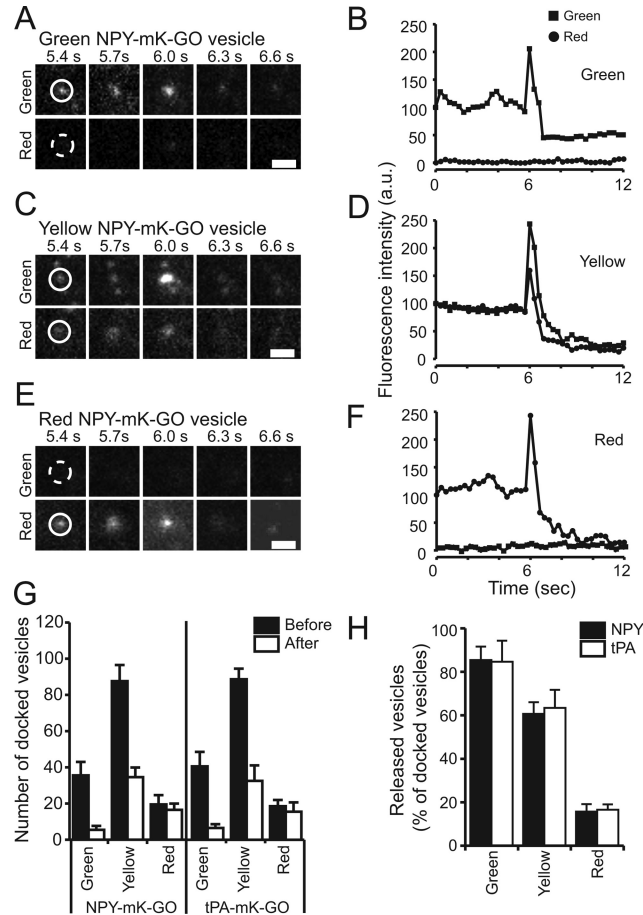
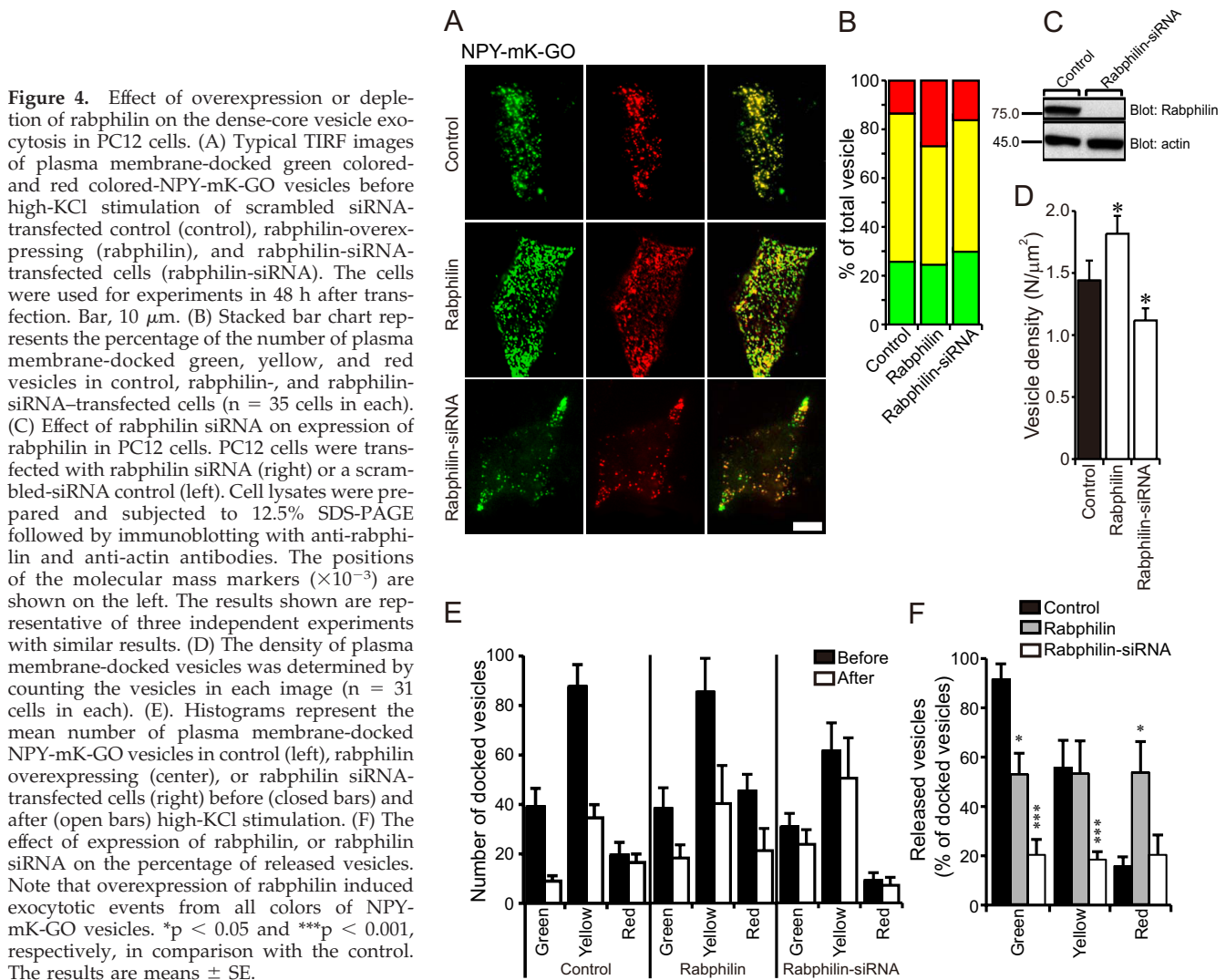


Figure 3. Exocytotic dynamics of dense-core vesicle cargoes NPY and tPA. Five sequential dual color TIRF images show the behavior of single green colored- (A), yellow colored- (C), and red-colored NPY-mK-GO (E) vesicles after applying 70 mM KCl to the cell. The cells were used for experiments in 48 h after transfection. The vesicle position before exocytosis is outlined by a circle. Bars, 1 μm . Fluorescence intensity traces are shown of vesicles containing both green colored- (B), yellow colored- (D), and red colored-NPY-mK-GO vesicles (F). (G) A histogram represents the mean number of plasma membrane-docked NPY-mK-GO vesicles (left; $n = 31$ cells) or tPA-mK-GO (right; $n = 28$ cells) vesicles per cell before (closed bars) and after (open bars) high-KCl stimulation. (H) Percentage of the number of NPY- or tPA-mK-GO release events during 5-min stimulation to the number of plasma membrane-docked vesicles before stimulation. Note that red colored-NPY- or tPA-mK-GO vesicles showed only few exocytotic events. The results are means \pm SE.

Overexpression or Depletion of Rabphilin Disturbed the Preferential Exocytosis on Its Age

We have demonstrated previously that both overexpression of rabphilin and Slp4-a greatly increased the number of plasma membrane-docked vesicles. Overexpression of rabphilin facilitated high-KCl-induced NPY-Venus release (Tsuboi and Fukuda, 2005; Tsuboi *et al.*, 2007), whereas overexpression of Slp4-a did not (Tsuboi and Fukuda, 2006b). These data indicated that both rabphilin and Slp4-a promote the docking of dense-core vesicles to the plasma membrane, but the function of those proteins on the dense-core vesicle exocytosis is completely opposite. We therefore used NPY-mK-GO probe to elucidate the functional difference between rabphilin and Slp4-a on the dense-core vesicle exocytosis.



Overexpression of rabphilin increased plasma membrane-docked vesicles (Figure 4, A and D), especially red vesicles (Figure 4B), whereas knockdown of endogenous rabphilin by siRNA (Figure 4C) decreased the number of plasma membrane-docked vesicles revealed by TIRF microscope (Figure 4, A and D). However, it is possible that overexpression of rabphilin affects the distribution of green- and red-colored vesicles inside of the cells. To check this possibility, we observed the vesicle color under the confocal microscope. As we expected, no differences in the population of green- and red-colored vesicle were observed in the overexpression or depletion of rabphilin (Supplemental Figure 3, A–C).

A previous report demonstrated that newly assembled vesicles were immobile at the plasma membrane and older vesicles were located deeper in the cell (Duncan *et al.*, 2003). Therefore, the overexpression of rabphilin seems to enhance the transport of old red vesicles located deeper in the cell to the plasma membrane. In contrast, no significant differences between the ratio of plasma membrane-docked vesicles of each color in control cells and in rabphilin-depleted cells (Figure 4B) revealed that depletion of endogenous rabphilin decreased the number of plasma membrane-docked vesicles of all colors (Figure 4E). These data suggest that the plasma membrane-docked vesicles were bound to rabphilin

for transport regardless of its age; therefore, the decreased number of vesicles on the plasma membrane by depletion of endogenous rabphilin seems to be unrelated to vesicle age. We also found that exocytotic responses occurred mainly from plasma membrane-docked green- and yellow-colored vesicles in NPY-mK-GO-expressing control cells. Interestingly, overexpression of rabphilin increased the exocytotic response from yellow- and red-colored vesicles but not green-colored vesicles, whereas depletion of endogenous rabphilin inhibited the exocytotic response from all-colored vesicles (Figure 4F). These data suggest that overexpression or depletion of rabphilin inhibited the preferential newly synthesized dense-core vesicle exocytosis. Our results also indicated that plasma membrane-docked vesicles in rabphilin-overexpressed cells are more readily released than those in rabphilin-depleted cells (Figure 4F). Previous studies suggested that exocytosis occurred at specific sites on the plasma membrane because of the inhomogeneous distribution of SNARE proteins (i.e., syntaxin1-a) (Ohara-Imaizumi *et al.*, 2007). Therefore, the dense-core vesicles in rabphilin-depleted cells might not be recruited to the right place on the plasma membrane where the exocytosis machinery exists. Conversely, the newly synthesized green vesicles in rabphilin-overexpressed cells might not always be existed in the

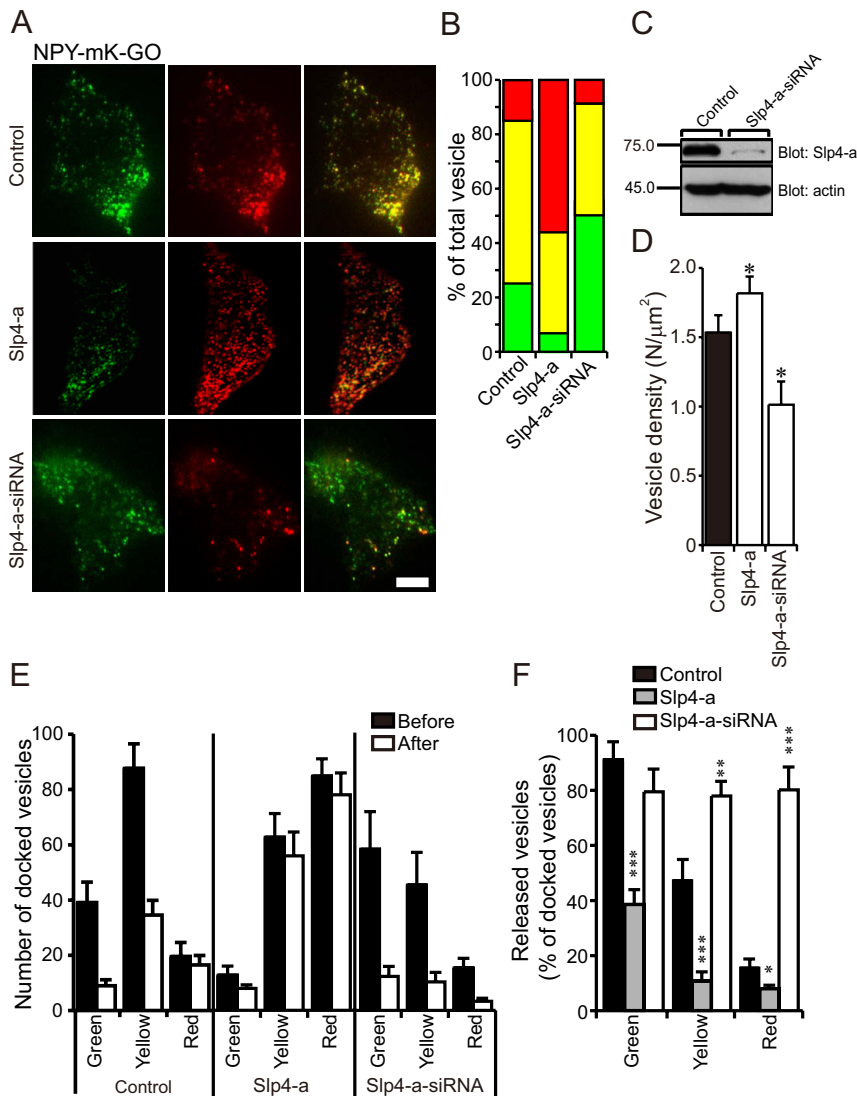


Figure 5. Effect of overexpression of Slp4-a or Slp4-a-siRNA expression on the dense-core vesicle exocytosis in PC12 cells. (A) Typical TIRF images of plasma membrane-docked green colored- and red colored-NPY-mK-GO vesicles before high-KCl stimulation of scrambled siRNA-transfected control (control), Slp4-a-transfected (Slp4-a), and Slp4-a-siRNA-transfected cells (Slp4-a-siRNA). The cells were used for experiments in 48 h after transfection. Bar, 10 μm. (B) Stacked bar chart represents the percentage of the number of plasma membrane-docked green, yellow, and red vesicles in control, Slp4-a, and Slp4-a-siRNA-transfected cells (n = 25 cells in each). (C) Effect of Slp4-a siRNA on expression of Slp4-a in PC12 cells. PC12 cells were transfected with Slp4-a-siRNA (right) or a scrambled-siRNA control (left). Cell lysates were prepared and subjected to 12.5% SDS-PAGE followed by immunoblotting with anti-Slp4-a and anti-actin antibodies. The positions of the molecular mass markers ($\times 10^{-3}$) are shown on the left. The results shown are representative of three independent experiments with similar results. (D) The density of plasma membrane-docked vesicles was determined by counting the vesicles in each image (n = 25 cells in each). (E) Histograms represent the mean number of plasma membrane-docked NPY-mK-GO vesicles in control (left), Slp4-a overexpression (center), or Slp4-a-siRNA-transfected cells (right) before (closed bars) and after (open bars) high-KCl stimulation. (F) The effect of expression of Slp4-a or Slp4-a siRNA on the percentage of released vesicles. Note that Slp4-a siRNA increased the number of plasma membrane-docked green-colored NPY-mK-GO vesicles and facilitated the yellow- and red-colored NPY-mK-GO release events. *p < 0.05, **p < 0.01, and ***p < 0.001, respectively, in comparison with the control. The results are means \pm SE.

right exocytotic place because yellow or red old vesicles have already been there. Together, these findings suggest that rabphilin regulates the transport of newly synthesized dense-core vesicles to right place on the plasma membrane.

Silencing of Slp4-a Increased the Number of Older Vesicle Exocytosis

We next observed the effect of overexpression or depletion of Slp4-a on the age-dependent preferential exocytosis. Overexpression of Slp4-a significantly increased the number of plasma membrane-docked NPY-mK-GO vesicles (Figure 5, A and D), whereas depletion of Slp4-a expression by siRNA (Figure 5C) had the opposite effect (Figure 5, A and D), suggesting that Slp4-a promotes the docking step in exocytosis. Interestingly, overexpression of Slp4-a increased the number of plasma membrane-docked red-colored NPY-mK-GO vesicles (Figure 5, A, Slp4-a panels, and B), whereas Slp4-a siRNA-transfected cells had increased numbers of plasma membrane-docked green-colored NPY-mK-GO vesicles (Figure 5, A, Slp4-a-siRNA panels, and B). Because Slp4-a inhibits the fusion step in exocytosis, unreleased vesicles stayed on the plasma membrane. Subsequently, the vesicles get older and become red-colored. In contrast, the

depletion of endogenous Slp4-a promotes the fusion step on exocytosis; therefore, only newly assembled green-colored vesicles are present on the plasma membrane (Figure 5E). Meanwhile, consistent with overexpression and depletion of rabphilin, no differences in the population of green and red-colored vesicle were observed in the overexpression or depletion of Slp4-a (Supplemental Figure 3, D and E).

NPY-mK-GO vesicle releasing events, involving vesicles of all colors, were decreased in Slp4-a overexpressing cells (Figure 5F), suggesting that exogenous Slp4-a was bound to both new and old vesicles, and inhibited the fusion of all colored secretory vesicles. In contrast, the release of old red vesicles were increased in Slp4-a depleted PC12 cells (Figure 5F), indicating that endogenous Slp4-a was bound to older vesicles to inhibit the fusion of secretory vesicles. Taken together, these findings suggest that Slp4-a regulates age-dependent preferential exocytosis by inhibiting the release of old vesicles.

DISCUSSION

In the present study, we demonstrate that NPY- or tPA-mK-GO is functionally targeted to the dense-core vesicles in PC12 cells, whereas NPY-timer (i.e., DsRed-E5) is not (Fig-

ure 2). Previous reports have shown that the fluorescent timer protein fused to ANF-timer was functionally targeted to secretory vesicles in bovine adrenal chromaffin cells and that the vesicles carrying ANF-timer were exocytosed functionally by high-KCl stimulation (Duncan *et al.*, 2003). The difference of targeting efficiency between our present data and previous reports could result from the distinct character of the cells and/or secretory vesicles derived from different cell lines. Generally, the dense-core vesicles store and release chromogranins and secretogranins (also known as “granins”), a unique group of acidic, soluble secretory proteins (O’Connor and Frigon, 1984). Several granins undergo aggregation induced by low pH and high calcium levels and interact with other components of the matrix of the dense-core vesicles, such as catecholamines, serotonin, and histamine (Kim *et al.*, 2001). Because pH and calcium concentrations in the Golgi complex varies depending on the cell type (Dannies, 2002), the tetrameric fluorescent timer protein might produce aggregates in PC12 cells, but not in bovine adrenal chromaffin cells. As a result, the aberrant folding of timer fluorescent protein disturbs the proper processing of the proNPY and/or sorting at the *trans*-Golgi network into maturing secretory vesicles in PC12 cells (Molinete *et al.*, 2000).

How can the preferential recruitment of rabphilin to newly synthesized vesicles be established? It has been shown that Rab3A and Rab27A are recruited to immature vesicles shortly after budding and are associated preferentially with newly synthesized vesicles (Handley *et al.*, 2007). Because rabphilin is bound to Rab3A and Rab27A as an effector, rabphilin consequently might be recruited to newly synthesized vesicles via Rab3A and Rab27A. However, it has been also shown that rabphilin transiently associates with the actin cytoskeleton via the actin-binding protein α -actinin (Kato *et al.*, 1996; Baldini *et al.*, 2005) and rapidly exchanges between the dense-core vesicles and cytosol (Handley and Burgoyne, 2008). Therefore, the association of rabphilin to Rab3A and/or Rab27a is not sufficient to explain the mechanism of rabphilin recruitment to the newly synthesized vesicles. Another explanation is that vesicles lose the binding ability to rabphilin in a time-dependent manner. Although several molecules are bound to vesicles to regulate exocytosis, vesicles have a limited number of rabphilin binding sites (i.e., Rab3A and Rab27A) on their surfaces. The newly synthesized vesicles have more rabphilin binding sites than the old vesicles because new vesicles have fewer chances to encounter other vesicle-binding molecules. After all, rabphilin is recruited to newly synthesized vesicles, and facilitates the transport of the new vesicles to the plasma membrane to promote age-dependent preferential exocytosis.

Knockdown of endogenous Slp4-a by specific siRNA decreased the number of plasma membrane-docked NPY- or tPA-mK-GO vesicles and induced exocytosis from both newer and older NPY- and tPA-mK-GO vesicles (Figure 5). Interestingly, Slp4-a-deficient mice whose pancreatic β cells contained a decreased number of attached vesicles on the plasma membrane, exhibited increased insulin secretion activity (Gomi *et al.*, 2005; Kasai *et al.*, 2008). Thus, it is likely that the mechanism of preferential exocytosis by vesicle age is conserved in insulin secretion on pancreatic β cells as well as in other neuroendocrine cells. Previous studies have also shown that chronic exposure of pancreatic β cells to high glucose decreased the expression of granuphilin/Slp4 (Abderrahmani *et al.*, 2006), and that granuphilin/Slp4 is involved in impaired insulin secretion in diabetic mice (Kato *et al.*, 2006). Accordingly, preferential exocytosis is a potential therapeutic target for treatment of diabetes mellitus.

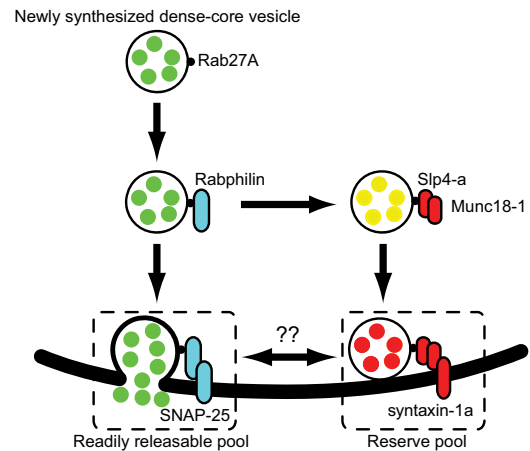


Figure 6. Proposed model for Slp4-a/rabphilin-dependent preferential dense-core vesicle exocytosis in neuroendocrine cells. Rabphilin and Slp4-a promote docking of dense-core vesicles to the plasma membrane through interaction with SNAP-25 (Tsuboi and Fukuda, 2005; Tsuboi *et al.*, 2007) and Munc18-1/syntaxin-1a complex (Tsuboi and Fukuda, 2006b), respectively. Dense-core vesicles docked to the plasma membrane by the rabphilin/SNAP-25 complex (blue bars) undergo preferential exocytosis (presumably corresponds to the readily releasable pool), whereas dense-core vesicles docked to the plasma membrane by the Slp4-a/Munc18-1/syntaxin-1a complex (red bars) do not undergo exocytosis (corresponds to the reserve pool). The molecular switch between readily releasable pool and reserve pool is currently unknown. Green-, yellow-, and red-colored vesicles correspond to newly synthesized vesicles, middle-aged vesicles, and old vesicles, respectively.

Based on our present findings, we propose following model for preferential exocytosis in neuroendocrine cells (Figure 6): 1) rabphilin is targeted to Rab27A on the newly synthesized dense-core vesicles; 2) rabphilin-attached dense-core vesicle is then transported to the plasma membrane; and 3) incidentally, rabphilin directly binds to SNAP-25 in the plasma membrane. The resulting Rab27A–rabphilin–SNAP-25 complex links the dense-core vesicles to the plasma membrane and enhances exocytotic events (Tsuboi and Fukuda, 2005). This route presumably corresponds to the “readily releasable pool” for the dense-core vesicle exocytosis. However, in some cases, rabphilin-attached dense-core vesicles cannot bind to SNAP-25. This vesicle will follow different route: 4) rabphilin detaches from Rab27A on the middle-aged dense-core vesicles; 5) Slp4-a, other Rab27A effector, occupies Rab27A on the dense-core vesicles, instead of rabphilin; and 6) Slp4-a simultaneously interacts with Rab27A and Munc18-1 on the dense-core vesicle and with closed-form syntaxin-1a, which does not contribute to SNARE complex formation, on the plasma membrane. The resulting quadripartite protein complex (i.e., Rab27A–Slp4-a–Munc18-1–syntaxin-1a) forms a tight complex between the dense-core vesicle and plasma membrane and inhibits high-KCl-induced exocytosis (Tsuboi and Fukuda, 2006b). This route presumably corresponds to the “reserve pool” for the dense-core vesicle exocytosis. Because the vesicle could not detach from the plasma membrane, the vesicles bound to Slp4-a subsequently become old. Although disassembly of the quadripartite protein complex must be necessary for the dense-core vesicle exocytosis, when and how the quadripartite protein complex disassembles remains completely unknown (Figure 6).

In summary, we demonstrate by live cell TIRF imaging combined with the use of new fluorescent timer probes that

Slp4-a and rabphilin regulate the segregation of dense-core vesicles according to vesicle age. We propose that rabphilin works as a molecular filter for segregation of readily releasable pool from reserve pool and Slp4-a as a molecular filter for segregation of reserve pool from readily releasable pool.

ACKNOWLEDGMENTS

This work was supported in part by Ministry of Education, Culture, Sports and Technology of Japan (Grants-in-Aid for Young Scientists 18689008 and 21790197); by the Naito Foundation; by Research Foundation for Opto-Science and Technology; and by The Nakajima Foundation.

REFERENCES

- Abderrahmani, A., Cheviet, S., Ferdaoussi, M., Coppola, T., Waeber, G., and Regazzi, R. (2006). ICER induced by hyperglycemia represses the expression of genes essential for insulin exocytosis. *EMBO J.* *25*, 977–986.
- Axelrod, D. (1981). Cell-substrate contacts illuminated by total internal reflection fluorescence. *J. Cell Biol.* *89*, 141–145.
- Baldini, G., Martelli, A. M., Tabellini, G., Horn, C., Machaca, K., Narducci, P., and Baldini, G. (2005). Rabphilin localizes with the cell actin cytoskeleton and stimulates association of granules with F-actin cross-linked by α -actinin. *J. Biol. Chem.* *280*, 34974–34984.
- Cheviet, S., Waselle, L., and Regazzi, R. (2004). Noc-king out exocrine and endocrine secretion. *Trends Cell Biol.* *14*, 525–528.
- Dannies, P. S. (2002). Mechanisms for storage of prolactin and growth hormone in secretory granules. *Mol. Genet. Metab.* *76*, 6–13.
- Duncan, R. R., Greaves, J., Wiegand, U. K., Matskevich, I., Bodammer, G., Apps, D. K., Shipston, M. J., and Chow, R. H. (2003). Functional and spatial segregation of secretory vesicle pools according to vesicle age. *Nature* *422*, 176–180.
- Fukuda, M. (2005). Versatile role of Rab27 in membrane trafficking: focus on the Rab27 effector families. *J. Biochem.* *137*, 9–16.
- Gomi, H., Mizutani, S., Kasai, K., Itohara, S., and Izumi, T. (2005). Granuphilin molecularly docks insulin granules to the fusion machinery. *J. Cell Biol.* *171*, 99–109.
- Handley, M. T., and Burgoyne, R. D. (2008). The Rab27 effector Rabphilin, unlike Granuphilin and Noc2, rapidly exchanges between secretory granules and cytosol in PC12 cells. *Biochem. Biophys. Res. Commun.* *373*, 275–281.
- Handley, M. T., Haynes, L. P., and Burgoyne, R. D. (2007). Differential dynamics of Rab3A and Rab27A on secretory granules. *J. Cell Sci.* *120*, 973–984.
- Jahn, R., and Sudhof, T. C. (1999). Membrane fusion and exocytosis. *Annu. Rev. Biochem.* *68*, 863–911.
- Karasawa, S., Araki, T., Nagai, T., Mizuno, H., and Miyawaki, A. (2004). Cyan-emitting and orange-emitting fluorescent proteins as a donor/acceptor pair for fluorescence resonance energy transfer. *Biochem. J.* *381*, 307–312.
- Kasai, K., Fujita, T., Gomi, H., and Izumi, T. (2008). Docking is not a prerequisite but a temporal constraint for fusion of secretory granules. *Traffic* *9*, 1191–1203.
- Kato, M., Sasaki, T., Ohya, T., Nakanishi, H., Nishioka, H., Imamura, M., and Takai, Y. (1996). Physical and functional interaction of rabphilin-3A with α -actinin. *J. Biol. Chem.* *271*, 31775–31778.
- Kato, T., *et al.* (2006). Granuphilin is activated by SREBP-1c and involved in impaired insulin secretion in diabetic mice. *Cell Metab.* *4*, 143–154.
- Kim, T., Tao-Cheng, J. H., Eiden, L. E., and Loh, Y. P. (2001). Chromogranin A, an “on/off” switch controlling dense-core secretory granule biogenesis. *Cell* *106*, 499–509.
- Molinete, M., Lilla, V., Jain, R., Joyce, P. B., Gorr, S. U., Ravazzola, M., and Halban, P. A. (2000). Trafficking of non-regulated secretory proteins in insulin secreting (INS-1) cells. *Diabetologia* *43*, 1157–1164.
- Nagai, T., Ibata, K., Park, E. S., Kubota, M., Mikoshiba, K., and Miyawaki, A. (2002). A variant of yellow fluorescent protein with fast and efficient maturation for cell-biological applications. *Nat. Biotechnol.* *20*, 87–90.
- O'Connor, D. T., and Frigon, R. P. (1984). Chromogranin A, the major catecholamine storage vesicle soluble protein. Multiple size forms, subcellular storage, and regional distribution in chromaffin and nervous tissue elucidated by radioimmunoassay. *J. Biol. Chem.* *259*, 3237–3247.
- Ohara-Imaizumi, M., Fujiwara, T., Nakamichi, Y., Okamura, T., Akimoto, Y., Kawai, J., Matsushima, S., Kawakami, H., Watanabe, T., Akagawa, K., and Nagamatsu, S. (2007). Imaging analysis reveals mechanistic differences between first- and second-phase insulin exocytosis. *J. Cell Biol.* *177*, 695–705.
- Rothman, J. E. (1994). Mechanisms of intracellular protein transport. *Nature* *372*, 55–63.
- Sawano, A., and Miyawaki, A. (2000). Directed evolution of green fluorescent protein by a new versatile PCR strategy for site-directed and semi-random mutagenesis. *Nucleic Acids Res.* *28*, E78.
- Tersikh, A., *et al.* (2000). “Fluorescent timer”: protein that changes color with time. *Science* *290*, 1585–1588.
- Tersikh, A. V., Fradkov, A. F., Zaraisky, A. G., Kajava, A. V., and Angres, B. (2002). analysis of DsRed mutants. Space around the fluorophore accelerates fluorescence development. *J. Biol. Chem.* *277*, 7633–7636.
- Tomas, A., Meda, P., Regazzi, R., Pessin, J. E., and Halban, P. A. (2008). Munc 18-1 and granuphilin collaborate during insulin granule exocytosis. *Traffic* *9*, 813–832.
- Tsuboi, T., and Fukuda, M. (2005). The C2B domain of rabphilin directly interacts with SNAP-25 and regulates the docking step of dense core vesicle exocytosis in PC12 cells. *J. Biol. Chem.* *280*, 39253–39259.
- Tsuboi, T., and Fukuda, M. (2006a). Rab3A and Rab27A cooperatively regulate the docking step of dense-core vesicle exocytosis in PC12 cells. *J. Cell Sci.* *119*, 2196–2203.
- Tsuboi, T., and Fukuda, M. (2006b). The Slp4-a linker domain controls exocytosis through interaction with Munc18-1/Syntaxin-1a complex. *Mol. Biol. Cell* *17*, 2101–2112.
- Tsuboi, T., and Fukuda, M. (2007). Synaptotagmin VII modulates the kinetics of dense-core vesicle exocytosis in PC12 cells. *Genes Cells* *12*, 511–519.
- Tsuboi, T., Kanno, E., and Fukuda, M. (2007). The polybasic sequence in the C2B domain of rabphilin is required for the vesicle docking step in PC12 cells. *J. Neurochem.* *100*, 770–779.
- Tsuboi, T., McMahon, H. T., and Rutter, G. A. (2004). Mechanisms of dense core vesicle recapture following “kiss and run” (“cavcapture”) exocytosis in insulin-secreting cells. *J. Biol. Chem.* *279*, 47115–47124.
- Tsuboi, T., and Rutter, G. A. (2003). Multiple forms of “kiss-and-run” exocytosis revealed by evanescent wave microscopy. *Curr. Biol.* *13*, 563–567.
- Tsuboi, T., Zhao, C., Terakawa, S., and Rutter, G. A. (2000). Simultaneous evanescent wave imaging of insulin vesicle membrane and cargo during a single exocytotic event. *Curr. Biol.* *10*, 1307–1310.
- Tsutsui, H., Karasawa, S., Shimizu, H., Nukina, N., and Miyawaki, A. (2005). Semi-rational engineering of a coral fluorescent protein into an efficient high-lighter. *EMBO Rep.* *6*, 233–238.
- Varadi, A., Tsuboi, T., and Rutter, G. A. (2005). Myosin Va transports dense core secretory vesicles in pancreatic MIN6 β -cells. *Mol. Biol. Cell* *16*, 2670–2680.
- Zerial, M., and McBride, H. (2001). Rab proteins as membrane organizers. *Nat. Rev. Mol. Cell Biol.* *2*, 107–117.